Fire Technology

Manufactured in The United States
https://doi.org/10.1007/s10694-021-01159-1

Effects of Fuel Depth and Pan Wall Material for Unsteady Pool Fires with Different Fuels

A. Shiva Kumar, H. S. Mukunda and C. S. Bhaskar Dixit, Fire and Combustion Research Centre, Jain (Deemed to be) University, Kanakapura Road, Bangalore, India*

Received: 16 March 2021/**Accepted:** 16 July 2021

Abstract. With the aim of providing a generalized dimensionless correlation for pan fuel burn fluxes, this work treats all the earlier work in this area and the data on specific experiments on a small pool fire performed in this study with fuels namely, kerosene, diesel, methanol and ethanol. The experiments were performed in stainless steel and mild steel pans of 0.2 m diameter and 40 mm depth with fuel depths up to 20 mm without water in an indoor fire laboratory. Data on temporal evolution of mass burn, pan wall temperatures, fuel temperatures and gas phase temperatures at specific height from the fuel surface have been obtained from the experiments and the behavior of the burn process has been delineated. The dimensionless correlation of the pool burn flux as a function of the geometric and thermodynamic properties of the pan and thermo-chemical properties of the fuels developed for n-heptane by the present authors recently has been examined for its validity for other fuels and shown to be good to with in ± 5% for the range of fuels, pan diameters and fuel depths.

Keywords: Pan fire, Burn rate, Scaling laws

List of Symbols

Al, *GL*	Aluminum alloy and glass
d_{pan}	Pan diameter (m)
h_{pan}, h_{fu}	Pan height, fuel depth (m)
h_{fb}, h_{wr}	Free board and water depth (m)
$h_{g,conv}$	Gas phase convective heat transfer coefficient (kW/m^2 K)
L_{fu}	Latent heat of vaporization of the fuel (kJ/kg)
k_w	Thermal conductivity of pan material (kW/m K)
$\dot{m}''_{fu}$	Mean mass flux (g/m^2 s)
M_{pc}	Dimensionless pan burn number
MS, *SS*	Mild steel, stainless steel
P_1, P_2, P_3	Dimensionless parameters as in Eqs. 1–3
T_f, T_s, T_{bfu}	Flame and fuel surface temperatures and fuel boiling point (K)
ρ_{fu}	Fuel density (kg/m^3)

*Correspondence should be addressed to: A. Shiva Kumar, E-mail: shivakumarannaiappa@gmail.com

Published online: 24 July 2021

1. Introduction

Pool fire has been a subject of study for six decades from the time [12] published a review of the Russian work. The research conducted can be broadly classified into steady and unsteady modes. In the unsteady mode, the pan is filled with a fixed amount of fuel and as burn proceeds the depth drops. Wall conduction brings in heat to the fuel and the fuel temperature continues to increase till the entire fuel reaches boiling stage. This last stage is called bulk boiling. The transition to bulk boiling involves distinct stages that have been experimentally delineated by Chen and colleagues [6, 7]. These authors have also presented the results for burn flux dependence on the initial temperature of n-heptane. The burn flux achieved during the bulk boiling stage is very high. In contrast, in steady state experiments [1, 4, 9, 17] a constant fuel level will be maintained throughout the experiments by continuously replenishing the fuel at a rate equal to the mass burn rate of the pool. In this method the pool has a certain depth towards the bottom of which, the fuel is maintained at a constant initial temperature. Because of this feature, the fuel is not allowed to reach the bulk boiling stage. The presence of a temperature profile limits the burn flux even if the fuel depth is increased by using a pan of larger depth.

The data from nineteen investigations on the burn flux as a function of pan diameter and fuel depth covering five fuels for both steady and unsteady modes of operation have been presented in Table 1. One important inference from this table is that the burn flux is always on the higher side in the unsteady mode of operation at comparable pan diameter and fuel depth. Fuel depth has effect on the burn flux for both steady and unsteady cases. For methanol and ethanol, burn flux seems capped at low values for all diameters with ethanol showing about 30% higher burn flux. In the case of other fuels, burn flux increases to large values with the pan diameter and fuel depth.

It is important to bring out that [9] have presented experimental results on a number of fuels and their mixtures using a steady approach and presented an empirical correlation. This correlation does not include fuel depth effect and does not account for all the fuel properties (like boiling point, for instance). Recently, [22] have conducted experiments on n-heptane for a range of pan diameters, and in the case of smaller pans (0.2 m), using different materials of the pan, namely, glass, stainless steel, mild steel and aluminum chosen for the increasing order of their thermal conductivity and with different fuel depths. One important finding is that the burn flux is very large at larger fuel depths essentially because of bulk boiling that occurs due to conductive heat transfer. This study also examined the relative role of conductive and convective modes of heat transfer dominant in small pans along the lines of [6, 7] and obtained a dimensionless correlation for predicting the burn flux as a function of the geometric and thermodynamic parameters of the pan and thermo-chemical parameters for n-heptane. The present paper extends the study to other fuels to examine the validity of the approach for other fuels such as methanol, ethanol, kerosene and diesel.

Table 1
Mass Burn Rate Comparison of Steady and Unsteady State Pool Fires

Fuel	Type	Size (shape) (m)	Fuel depth (mm)	Burn flux (g/m^2s)	References
Methanol	Ste	0.1–0.6,C	63.0–147.0	14–15	[a, b, c, f, g, & p]
	Ste	1.0, C	63.5	19	[p]
	Ste	2.0, C	63.5	21	[m]
	Uns	1.2–2.4, C	76.0	20–21	[d]
Ethanol	Ste	0.25–1.0, C	63.5	13–24	[p]
	Uns	0.24–0.33, S	30.0	20–22	[o]
	Ste	0.3, C	145.0	16	[g]
	Ste	0.5–2.0, C	–	18–27	[h]
	Ste	2.0, C	63.5	27	[m]
Diesel	Ste	0.15–2.6, C	–	10–50	[a]
	Ste	0.5–1.0,C	–	28–40	[l]
	Uns	1.5–4.0, C	5.5–8.1	32–56	[i]
Kerosene	Ste	0.15–22.9, C	–	12–50	[a]
	Uns	30.0–50.0, C	–	65	[e]
Heptane	Uns	0.1–0.3, C	13.0	19–37	[j,n]
	Ste	0.2–0.25, S	26.0	16–21	[q]
	Uns	0.17–0.33, S	30.0	45–66	[o]
	Uns	0.2–2, C	5.0–30.0	10–75	[r]
	Ste	0.25–2.0, C	63.5	27–64	[m, p]
	Uns	0.27–0.33, S	10.0	23–24	[k]
	Ste	0.3, C	137.0	36	[f]
	Ste	0.6–1.0, C	87.0	57–66	[f]
	Ste	0.5–2.0, C	–	39–60	[h]
	Uns	1.2–1.7, C	76.0	68–73	[d]
	Uns	2.7–10.0, S,C	30.0	81–98	[e]

Ste = Steady, Uns = Unsteady, C = circular, S = Square, a = [2], b = [3], c = [1], d = [15], e = [16], f = [17], g = [13], h = [8], i = [5], j = [18], k = [19], l = [21], m = [4], n = [6, 7], o = [11], p = [9], q = [14] & r = [22]

2. Experimental Arrangement

The experimental arrangement is the same as in the earlier work [22] and consists of the pan mounted on a balance with a ceramic blanket in-between to ensure safety of the balance and has thermocouples fixed to select points on the wall and inside the liquid pool. Measurements consist of mass, wall temperatures, temperatures within the condensed phase and center line gas temperatures with time. The balance is of 5 kg capacity with an accuracy of 100 mg is used to measure the mass loss. K type thermocouples of bead size 0.4 mm are used to obtain the required temperatures. The pans of 200 mm internal diameter with 3 mm wall thickness, 40 mm depth made of mild steel and stainless steel are used to conduct the experiments for fuel thicknesses up to 20 mm. Diesel, kerosene, methanol and ethanol fuels are used in these experiments.

3. Thermal Properties of Wall Material and Fuel

While several thermal properties of the pan were obtained from data sheets, thermal conductivity which is a more sensitive property of the composition was experimentally obtained by measuring a one-dimensional temperature profile and extracting thermal conductivity from the data. The data matched with information from published sources. In specific cases, transient technique was adopted to measure the thermal conductivity of the sample pieces. Table 2 presents the data on the pan wall materials considered. If we make a simple estimate of the transient conduction times using $t_{cond} \sim h_{pan}^2/8\alpha_w$, we get the values set out in the last column. The transient conduction times are small compared to the burn time. This implies that steady conduction process along the wall will be a good approximation.

The thermodynamic and transport properties of the fuels tested are set out in Table 3. Thermal diffusivity of the liquid fuels are in the order of magnitude lower than the pan material and hence the heat transfer process through the liquid has to account for unsteady process. The value of T_f set out in Table 3 is the maximum centerline flame temperature at a height of 0.4 d_{pan} obtained from the experiments. The flame temperature plays an important role in the radiative flux received by the fuel surface and is used in a more detailed model of the prediction of mass versus time of various fuels. The measurement procedure is discussed in [22] in some detail and what has been followed here is to use heated thermocouple probe of 0.4 mm bead diameter in the flame. Very specifically, issues of sooting have been overcome through this procedure. Figure 1 shows the measured flame temperature for n-heptane, ethanol, kerosene and diesel fuels. The difference in the measured flame temperatures without and with heating is shown in the case of n-heptane. The presently measured mean values of T_f measured for diesel, methanol and ethanol are also set out in Table 3 and as can be seen are also in close agreement with the values reported in the literature and are correct to within $\pm$ 50°C.

4. Results

The comparison of the mass loss versus time of stainless steel pan and mild steel pan experiments with diesel and kerosene at fuel depths of 10 mm and 20 mm are set out in Fig. 2. In the case of diesel, the burn flux is nearly constant at a low level of 8 to 9 g/m^{2}s for the entire duration. This means that the heat received from conduction has little influence. Convection alone dominates the heat transfer process because radiation makes very little contribution at this pan size. The reason for this behavior is that for diesel, the boiling range is large and the liquid phase absorbs a lot of sensible heat over time and the boiling range is also so large that the liquid phase slowly gets reduced to lead to maintaining a low burn flux. For kerosene, however, the behavior is different. The initial mass loss is about 10 g/m^{2}s for both SS and MS pans and at later times, the higher wall heat

Table 2
Properties of Pan ($t_{cond} \sim h_{pan}^2/4\alpha_w/2$)

Material	d_{pan} (mm)	t_w (mm)	ρ_w (kg/m^3)	c_{pw} (kJ/kg K)	k_w (W/m K)	α_w (mm^2/s)	h_{pan} (mm)	t_{cond} (s)
MS	200	3	7800	0.46	32	8.9	40	22
SS	200	3	7800	0.46	16	4.5	40	44

Table 3
Properties of the Fuel

Fuel	ρ_{fu} (kg/m^3)	T_{bfu} (K)	c_{pfu} (kJ/kg K)	L_{fu} (kJ/kg)	k_{fu} (W/m K)	α_{fu} (mm^2/s)	μ_{fu} (mN s/m^2)	T_f (K)
n-heptane	680	369	2.1	322	0.14	0.09	0.41	1200
Kerosene	810	490	2.01	320	0.15	0.089	1.64	1150
Diesel	850	660	1.9	300	0.15	0.098	3.35	1100
Diesel [21]	–	–	–	–	–	–	–	1100
Ethanol	785	351	2.57	846	0.16	0.082	0.98	1350
Ethanol [10]	–	–	–	–	–	–	–	1310
Methanol	791	338	2.57	1100	0.20	0.093	0.51	1450
Methanol [23]	–	–	–	–	–	–	–	1434

transfer in the case of MS pan leads to higher burn flux compared to SS pan. The reason for the difference in behavior between diesel and kerosene is that diesel has components with much higher boiling range compared to kerosene and the heat transferred by conduction is unable to raise the temperature to levels allowing for higher vaporization rates. The behavior of kerosene is similar to that of n-heptane [22].

Figure 3 shows the mass loss with the time of 0.2 m diameter MS pan with 5, 10, and 20 mm depth for methanol and ethanol. The results are nearly identical and fuel depth has little effect. The initial mass burn rate at fuel depths is 11 g/m^{2}s and the higher flux of 17 g/m^{2}s is reached much earlier (as a fraction of total burn time) than in the case of kerosene and n-heptane [22] indicating that convection appears enhanced to larger values and conduction plays a very minor role (because the slope does not change during most of the time).

In order to explore the behavior of the fuels within the liquid phase, the temperatures of the liquid at 1 mm from the bottom are plotted against time in Fig. 4. For, n-heptane, ethanol and methanol which are pure fuels, the temperature reaches their respective boiling points and stays at that temperature till complete burnout occurs. This period of burn when the temperature has reached the boiling point is the bulk boiling condition discussed earlier. This duration is much

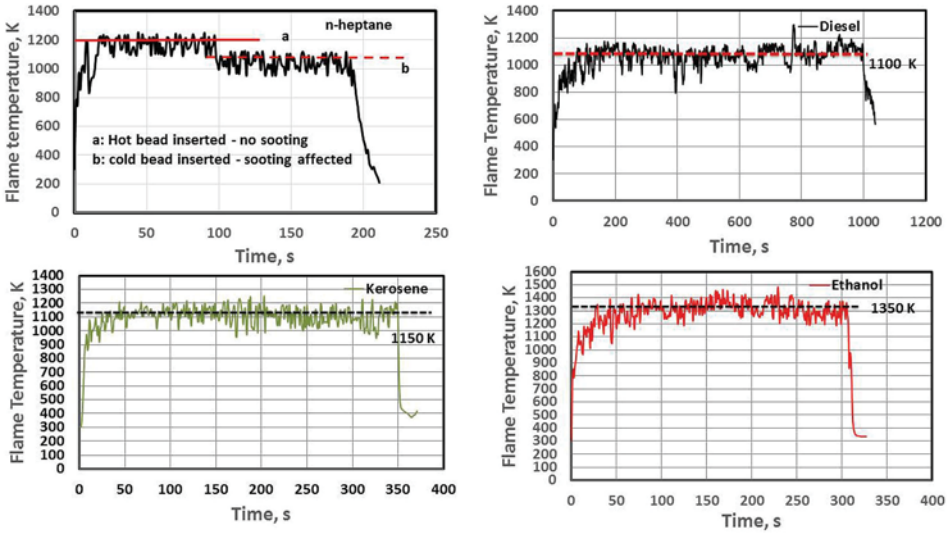

Figure 1. Centerline flame temperature at a height of 0.4 d_{pan} versus time for n-heptane, diesel, kerosene and ethanol fuels in 0.2 m diameter pool fire.

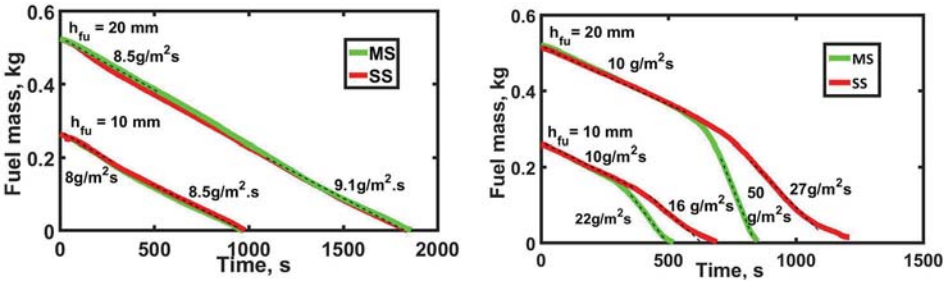

Figure 2. Comparison of mass loss with time for 0.2 m SS and MS pans, 40 mm deep with 10 and 20 mm diesel (left) at 27± 2°C and kerosene (right) at 24± 2°C initial temperature.

large for methanol and ethanol because their boiling points are lower than of n-heptane and their high latent heat of vaporization reduces the burn flux. In the case of kerosene and diesel, the temperature keeps on increasing with time till the end of the experiment, since they are fuels composed of various petroleum fractions. In the case of diesel, the temperatures go beyond 650 K indicating to evaporation of some heavy fragments in the fuel.

The data from various experiments conducted here are set out in Table 4. The mean flux ($\bar{\dot{m}}''_{fu}$) shown in this table is obtained as the ratio of the fuel mass divided by the burn time and pan cross sectional area. Also shown is the peak flux obtained from the increased burn rate after a couple of hundred seconds during

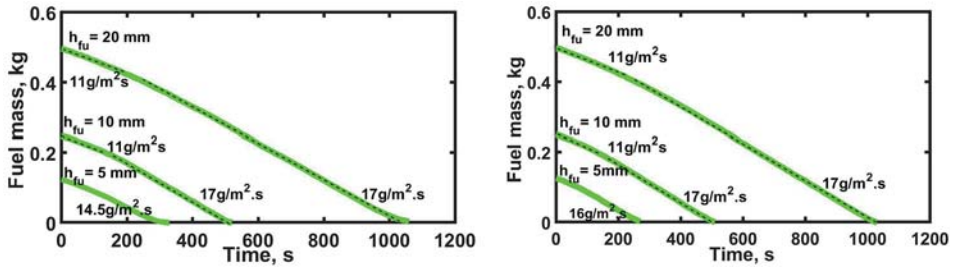

Figure 3. Mass loss versus time of ethanol (left) and methanol (right) in 0.2 m dia MS pan, 40 mm deep with 5, 10 and 20 mm fuel depths at 28 ± 2°C initial temperature.

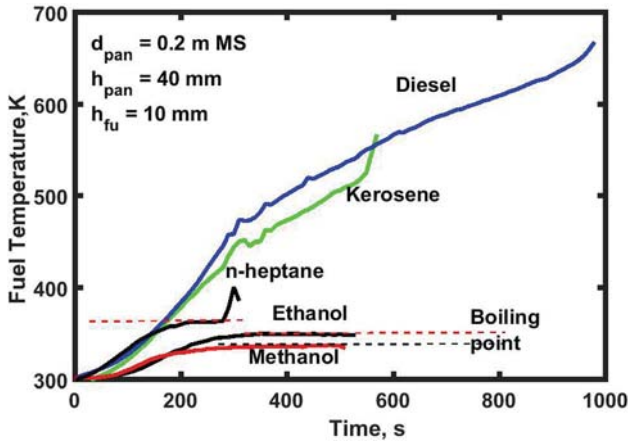

Figure 4. Centerline fuel temperature at 1mm from bottom of pan versus time for n-heptane, kerosene, diesel, ethanol and methanol fuel in 0.2 m dia MS pan, 40 mm deep with 10 mm fuel depth.

which the liquid heats up towards boiling with heat flux from the gas phase as well as wall conduction. What is clear from the table is that both the mean and peak flux increase with the depth with a tendency to reach asymptotic values for n-heptane. For kerosene, the mass flux increases with fuel depth but for diesel, ethanol, and methanol the increase of flux is not significant even though the depth of fuel is increased. Also, the material of the pan - MS or SS here matters significantly in terms of the burn behavior only for n-heptane and kerosene fuel.

5. The Correlation

The correlation that was evolved [22] using the fact that the burn flux (a) increases with the diameter of the pan (d_{pan}) reaching an asymptotic value, a feature that is embedded in classical expressions for extinction coefficient arising out of

Table 4
Mean and Peak Burn Fluxes (g/m^2s) for 0.2 m Dia Pan; Data Accurate to ± 5%

Flux for h_{fu} (mm) =	5	10	20	30
SS, n-heptane, mean	16.2	17.8	25	28.9
SS, n-heptane, peak	20.1	25.7	34.4	41
MS, n-heptane, mean	22.3	26.6	29.8	34
MS, n-heptane, peak	33.0	42.5	58.1	67.2
SS, kerosene, mean	–	11.8	13.6	–
SS, kerosene, peak	–	16.0	22.0	–
MS, kerosene, mean	–	15.6	19.4	–
MS, kerosene, peak	–	27.0	50.0	–
SS, diesel, mean	–	8.5	9.0	–
SS, diesel, peak	–	8.1	9.1	–
MS, diesel, mean	–	8.7	8.9	–
MS, diesel, peak	–	8.0	9.5	–
MS, ethanol, mean	12.0	15.2	15.0	–
MS, ethanol, peak	14.5	17.2	17.0	–
MS, methanol, mean	14.6	15.6	15.3	–
MS, methanol, peak	16.0	17.0	17	–

radiation domination at large sizes, (b) increases with the fuel depth (h_{fu}), a feature that was noted as important to be included for the dependence of burn flux as also the associated free board ($h_{fb} = h_{pan} - h_{fu}$), (c) depends on the latent heat (L_{fu}) and boiling point ($T_{b,fu}$) of the fuel to account for heat absorption into the liquid, (d) increases on the fuel temperature in relationship to its boiling point and (e) depends on the pan wall material thermal conductivity, (k_w).

Rendering conductive heat transfer coefficient, k_w/h_{pan} dimensionless is performed using the convective heat transfer coefficient, $h_{g,conv}$ that is obtained by expecting that the burn rate flux is controlled by convection in the early stages in a small diameter pan, in this case, 0.2 m diameter where radiation flux is minimal. This gives a value of 0.0045 kW/m^2K. Subsequent burn rate simulations using an unsteady code [20] have confirmed this result. With regard to other dimensions—fuel thickness, free board, pan diameter and pan wall thickness, several possible dimensionless constructions are possible. The candidate for rendering the pan diameter dimensionless should arise from free convective length scale, $[v_g^2/g]^{(1/3)}$, where $v_g = \mu_g/\rho_g$ is the dynamic viscosity of the hot gases. With μ_g = 1.8 $\times 10^{-5}$ kg/m s, g = acceleration due to gravity, 9.8 m/s^2, this length scale is 0.21 m. After some trials, the following choices were deduced.

$$P_1 = \left[\frac{k_w}{h_{pan}h_{g,conv}}\frac{h_{fu}}{h_{fb}}\right]^{1/4} \tag{1}$$

$$P_2 = \left[1 - \exp(-0.25(d_{pan}/0.21)^{1.5}/P_1)(1 + 0.1(h_{wr}/h_{pan})^{2.3})\right] \tag{2}$$

$$P_3 = \left[\frac{(T_{bfu} - T_0)}{(T_{bfu} - 300)}\frac{300}{T_{bfu}}\right]^{-0.35} \tag{3}$$

The parameter P_1 accounts for conductive flux in addition to fuel depth and associated free board effects, P_2 accounts for the effect of pan diameter and water on the mass burn rate (though in the present case experiments were performed without water, particularly because alcohols also were studied), and P_3 for initial temperature effects.

The dimensionless number is set out as

$$M_{pc} = P_1 P_3[1.5 + 8.5P_2] \tag{4}$$

The final expression for the burn flux becomes

$$\bar{m}''_{fu}(g/m^2 s) = M_{pc}\frac{(h_{g,conv}(T_f - T_{bfu})}{4L_{fu}} \tag{5}$$

where $h_{g,conv}$ is 4.5 W/m^{2}K. Figure 5 shows the comparison of experimental mass burn rate versus the predicted mass burn rate of diesel, kerosene, n-heptane, gasoline, methanol and ethanol fuels for a range of pan diameters, pan material, steady and unsteady experimental condition and at different fuel depths. These include the data of 78 experiments from present studies and 41 data set from literature. The root mean square error of the predictions in comparison to experiments is about 5% over a wide range of parameters of practical importance and the correlation appears very good. The sensitivity of the predicted burn flux to the parameters controlling it are set in Table 5. It can be seen that most sensitive parameter is the initial temperature of the fuel. The least sensitive parameter is the depth of water. Pan diameter around 2 m has little sensitivity because the most dominant heat flux—due to radiation does not change around and beyond this diameter.

6. Conclusions

The present study was initiated to understand the fuel depth and pan material effects on the burn flux for different fuels kerosene, diesel, ethanol, and methanol. From the experiments, it is found that the burn rate for kerosene increases with increasing fuel depth but for diesel, ethanol, and methanol the burn flux dependence on fuel depth is not significant. The burn flux for diesel fuel shows less dependence on the thermal conductivity of the pan used. The M_{pc} based correlation is capable of predicting the mean burn flux of various fuels for the experi-

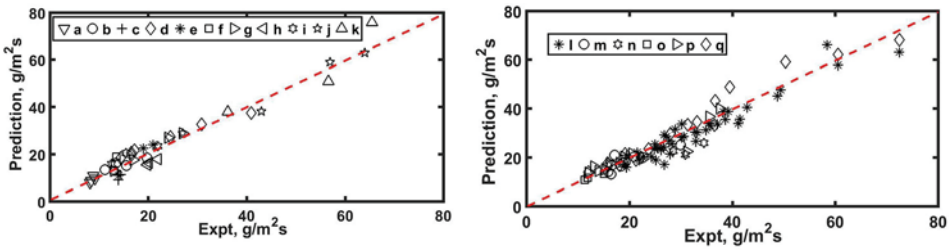

Figure 5. Experimental versus predicted burn flux of present studies and data from literature. (a = MS-SS-0.2D-Diesel present, b = MS-SS-0.2D-Kerosene present, c = MS-Ethanol present, d = GL-0.338-0.677D-Gasoline-[24], e = SS-0.25-2D-Methanol-[9], f = SS-MS-0.3-0.6D-[17], g = SS-0.25-2D-Ethanol-[9], h = MS-0.27-0.372D-Ethanol-[11], i = Gl-0.11-0.29D-Heptane-[14], j = SS-0.25-2D-Heptane-[9], k = MS-SS-0.3-1D-Heptane-[17], l = MS-0.2-2D-Heptane- [22], m = SS-0.2D-Heptane-[22], n = AL-0.2D-Heptane-[22], o = GL-0.2D-Heptane-[22], p = 0.1-0.2D-heptane-[6, 7], q = 0.2-2D-Heptane with water-[22].

Table 5
Sensitivity of Burn Flux, $\bar{m}''_{fu}$ to Various Parameter Changes Each by 10%

Parameter	%
Pan diameter at 0.2 m	4
Pan diameter at 0.5 m	7
Pan diameter at 2.0 m	1
Wall thermal conductivity	2
Fuel depth	2.5
Pan height	3.5
Freeboard	3.5
Fuel initial temperature at 300 K	22.0
Water depth at 10 mm	0.2

ments performed in both steady and unsteady experimental conditions at different fuel depths taking into account all the geometrical and thermo-chemical properties of fuels and pans used.

Acknowledgements

The authors are thankful to the authorities of Jain (Deemed to be)university for encouragement in the conduct of this research and we would like to thank the reviewers for their thoughtful comments which helped us in improving the paper.

References

1. Akita K, Yumoto T (1965) Heat transfer in small pools and rates of burning of liquid methanol. In: Tenth symposium (international) on combustion. The Combustion Institute, pp 943–948
2. Blinov VI, Khudiakov GN (1961) Diffusion burning of liquids. Report No. AD296762, Moscow Academy of Sciences, U S Army Engineering Research and Development Laboratories, Fort Belvoir, Virginia
3. Bugress DS, Strasser A, Grumer J (1961) Diffusive burning of liquid fuels in open trays. Fire Res Abstr Rev 3:177
4. Blanchet TK, Anttila JS (2011) Hydrocarbon characterization experiments in fully turbulent fires—results and data analysis. Report No. SAND2010-6377, Sandia National Laboratories, Albuquerque, NM
5. Chatris JM, Quintela J, Folch J, Planas E, Arnaldos J, Casal J (2001) Experimental study of burning rate in hydrocarbon pool fires. Combust Flame 126:1373–1383
6. Chen B, Lu S, Li C, Kang Q, Yuan M (2011) Unsteady burning of thin layer pool fires. J Fire Sci 30:3–15
7. Chen B, Lu S, Li C, Kang Q, Lecoustre V (2011) Initial fuel temperature effects on burning rate of pool fire. J Hazard Mater 188:369–374
8. De Ris JL, Wu PK, Heskestad G (2000) Radiation fire modeling. Proc Combust Inst 28:2751–2759
9. Ditch BD, de Ris JL, Blanchet TK, Chaos M, Bill RG Jr, Dorofeen SB (2013) Pool fires—an empirical correlation. Combust Flame 160:2964–2974
10. Fischer SJ, Duparc BH, Grosshandler WL (1987) The structure and radiation of an ethanol pool fire. Combust Flame 70:291–306
11. Fang J, Tu R, Guan JF, Wang JJ, Zhang YM (2011) Influence of low air pressure on combustion characteristics and flame pulsation frequency of pool fires. Fuel 90:2760–2766
12. Hottel HC (1958) Review, certain laws governing diffusive burning of liquids. Fire Res Abstr Rev 1:41–44
13. Hamin A, Fischer SJ, Kashiwagi T, Klassen ME, Gore JP (1994) Heat feedback to the fuel surface in pool fires. Combust Sci Technol 97:37–62
14. Hu L, Hu J, Liu S, Tang W, Zhang X (2015) Evolution of heat feedback in medium pool fires with cross air flow and scaling of mass burning flux by a stagnant layer theory solution. Proc Combust Inst 35:2511–2518
15. Kung HC, Stavrianidis P (1982) Buoyant plumes of large-scale pool fires. In: Nineteenth symposium international on combustion. The Combustion Institute, pp 905–912
16. Koseki H (1989) Combustion properties of large liquid pool fires. Fire Technol 25:241–255
17. Klassen M, Gore JP (1994) Structure and radiation properties of pool fires—Report No. NIST-GCR-94-651. National Institute of Standards and Technology, Gaithersburg
18. Kang Q, Lu S, Chen B (2009) Experimental study on burning rate of small scale heptane pool fires. Eng Thermophys 55:973–979
19. Li ZH, He Y, Zhang H, Wang J (2009) Combustion characteristics of n-heptane and wood crib fires at different altitudes. Proc Combust Inst 32:2481–2488
20. Mukunda HS, Shivakumar A, Sowriraajan AV, Bhaskar Dixit CS (2019) Unsteady pool fires—fuel depth and pan wall effects—experiments and modeling, FCRC report—1902, Fire and Combustion Research Center, Jain (Deemed-to-be-University), Bangalore

21. Sudheer S, Prabhu SV (2012) Measurement of flame emissivity of hydrocarbon pool fires. Fire Technol 48:183–217
22. Shiva Kumar A, Sowriraajan AV, Bhaskar Dixit CS, Mukunda HS (2021) Experiments on unsteady pool fires—effects of fuel depth, pan size and wall material. Sadhana 46:53
23. Weckman EJ, Strong AB (1996) Experimental investigation of the turbulence structure of medium scale methanol pool fires. Combust Flame 105:245–266
24. Zhao J, Huang H, Wang H, Zhao J, Liu Q, Li Y (2017) Experimental study on burning behaviors and thermal radiative penetration of thin-layer burning. J Therm Anal Calorim 130:1153–1162